1 ***GTP cyclohydrolase II* (*gch2*) and axanthism in ball pythons: a new vertebrate model for**

2 **pterin-based pigmentation**

3 *Alan Garcia-Elfring, °Heather L. Roffey, *Jaren M. Abergas, *Andrew P. Hendry, and *Rowan D.

4 H. Barrett

5 *Department of Biology, McGill University, Montreal, QC, Canada

6 °Biology Department, Vanier College, Montreal, QC, Canada

7

8

9 **Corresponding authors: rowan.barrett@mcgill.ca, alan.garcia-elfring@mail.mcgill.ca**

10

11

12

13

14

15

16

17

Abstract:

Pterin pigments are responsible for many of the bright colours observed across the animal kingdom. However, unlike melanin, the genetics of pterin-based pigmentation has received relatively little attention in animal colouration studies. Here, we investigate a lineage of axanthic ball pythons (*Python regius*) found in captivity as a model system to study pterin pigmentation in vertebrates. By crowdsourcing shed skin samples from commercial breeders and applying a case-control study design, we utilized whole-genome pool sequencing (pool-seq) and variant annotation. We identified a premature stop codon in the gene *GTP cyclohydrolase II* (*gch2*), which is associated with the axanthic phenotype. GCH2 catalyzes the first rate-limiting step in riboflavin biosynthesis. This study provides the first identification of an axanthism-associated gene in vertebrates and highlights the utility of ball pythons as a model to study pterin-based pigmentation.

INTRODUCTION

Animal pigmentation has long served as a valuable model for understanding genetics, development, and evolution (Cott 1940; Kronforst et al. 2012; Caro 2017; Endler et al. 2017; San-Jose et al. 2017). Vertebrate pigmentation arises from the differential absorption of light by pigments within specialized cells called melanophores (melanocytes in endothermic vertebrates) and xanthophores. All vertebrates produce a brown/black form of melanin derived from the amino acid tyrosine (Wakamatsu and Ito 2021). In addition, poikilothermic vertebrates (fish, amphibians, and reptiles) display bright colouration through yellow/red pigments found in cells called xanthophores. Xanthophores derive their vibrant yellow or red colouration from pterin or carotenoid pigments. While vertebrates acquire carotenoids exclusively from their diet (Maoka 2020), pterin pigments are synthesized de novo from guanosine triphosphate (GTP). Coloration can also be structural, with poikilothermic vertebrates using guanine nanocrystals in iridophore cells to generate structural colouration via the constructive interference of light. Although melanin-based pigmentation has been extensively studied, other pigment classes, such as pterins, have received less attention.

The mouse has been pivotal in studies of melanocyte biology, helping uncover the genes responsible for melanocyte development and patterning: *Kit*, *Pax3*, *Mitf*, *Edn3*, *Ednrb*, and *Sox10* (Steingrímsson et al. 2005); melanin synthesis: *Tyr*, *Tyrp1*, *Dct* (McNamara et al. 2021; Wakamatsu and Ito 2021); and its regulation, such as *Mc1r* (Garcia-Borron et al. 2005). Meanwhile, the zebrafish model has laid the foundation for understanding poikilothermic vertebrate pattern formation (Singh and Nüsslein-Volhard 2015). Studies on zebrafish have

58 shown that pattern formation arises from local, short- and long-range cell-cell interactions
59 between chromatophore types (Frohnhöfer et al. 2013). For example, zebrafish mutants lacking
60 any one of the chromatophores (iridophores, melanophores, and xanthophores) fail to develop
61 stripes and often develop spots instead. In double mutants lacking two of the three
62 chromatophore types, the remaining chromatophores uniformly cover the body (Frohnhöfer et
63 al. 2013; Owen et al. 2020). Gap junction proteins mediate these cell-cell interactions, and
64 mutations in these genes can result in labyrinthine patterning (Irion et al. 2014). However, it
65 remains unclear how widely zebrafish cell-cell interactions apply across vertebrate taxa.

66 First discovered in butterfly wings (Hopkins 1895), pterin-based pigmentation is
67 ubiquitous in nature but has received less attention compared to melanin-based pigmentation
68 (Andrade and Carneiro 2021). The pterin pigment synthesis pathway has been largely
69 elucidated through studies in *Drosophila* (Glassman and Mitchel 1959; Courtright 1967; Ziegler
70 and Harmsen 1970; Goto and Sugiura 1971; Evans and Howells 1978; Spradling and Rubin 1983;
71 Reaume et al. 1991; Kim et al. 2013). Notably, *Drosophila*'s first described mutant, "white,"
72 lacked eye pterin (drosopterin) and ommochrome pigments (Morgan 1910). While melanin is
73 often linked to adaptive phenotypes, such as cryptic colouration (Barrett et al. 2019; Harris et
74 al. 2020; Baltazar-Soares et al. 2024), pterin pigments are key in signaling both within and
75 between species (Kikuchi and Pfennig 2012; Kikuchi et al. 2014; Andrade and Carneiro 2021). In
76 vertebrates, zebrafish have been the primary model for studying xanthophore biology,
77 including xanthophore specification from neural crest cells (Kelsh et al. 1996; Odenthal et al.
78 1996; Parichy et al. 2000; Minchin and Hughes 2008) and pigment synthesis (Ziegler 2003; Lister
79 2019).

Studying mutants lacking a pigment can offer insights into bright colouration genetics, a strategy pioneered by Thomas Hunt Morgan with fruit flies. Axanthic animals, which lack yellow and red pigments but retain melanin, are rare among vertebrates. Only a few axanthic amphibians and reptiles have been discovered in nature (Bechtel 1991; Jablonski et al. 2014; Cattaneo 2015; Kolenda et al. 2017; Cavalcante and Bruni 2018; Borteiro et al. 2021; Schluckebier et al. 2022). Axanthic vertebrate models are also scarce in pigmentation research, with the axanthic axolotl, first described by Lyerla and Dalton (1971), being a notable exception (Dunson 1974; Frost et al. 1986; Bukowski et al. 1990; Masselink and Tanaka 2021). Axanthic axolotls lack both xanthophores and iridophores, meaning axanthism in axolotls affects chromatophore development rather than pigment synthesis. However, low survivability in axanthic axolotls presents challenges for research, including breeding programs, population genetics studies, and comparative analyses.

Here, we use a line of axanthic ball pythons to study the genetics of yellow pigmentation in reptiles. We hypothesize that, assuming a similar mechanism of vertebrate pattern formation to zebrafish (Frohnhöfer 2013; Singh and Nüsslein-Volhard 2015), axanthism in ball pythons results from defects in pterin pigment synthesis (Ziegler 2003), rather than carotenoid metabolism or xanthophore development. We expect that xanthophore development remains unaffected, as axanthic ball pythons exhibit wild-type melanin patterning, which suggests intact cell-cell interactions. Furthermore, we anticipate that yellow pigmentation (or its absence) is linked to pterin-based pigmentation, rather than carotenoids, since ball pythons are born with yellow colouration before acquiring carotenoids from their diet. This suggests that pterins, not carotenoids, underlie the colouration difference.

METHODS

Sample collection, study design, DNA extraction, and sequencing

We crowd-sourced ball python shed skin samples from breeders, including five samples with the recessive VPI Axanthic colour morph (Table S1). VPI refers to Vida Preciosa International, the reptile propagation company that first received the wild-caught axanthic snake from Western Africa and established the phenotype in captivity. All VPI Axanthic (hereafter referred to as 'axanthic') ball pythons descend from this individual.

Additionally, we collected 38 samples of the recessive 'Clown' phenotype (Table S2), which we used as a control for identifying candidate mutations linked to the axanthic trait. We also gathered samples from other colour morphs: 'Spider' (n=26, Table S3), 'Enchi' (n=7, Table S4), 'Ivory' (n=15, Table S5), and 'Lavender' (n=14, Table S6). These were used as further control sets because, according to breeder pedigrees, these morphs do not carry any axanthism variation.

Similarly, the axanthic samples were confirmed to lack any variation associated with the Clown, Spider, Enchi, Ivory, or Lavender morphs (i.e., inferred to be homozygous for the reference alleles at those loci). We identified candidate mutations by comparing genetic variation in the axanthic pool with multiple reference sample sets known, through pedigree analysis, to not carry the axanthic variant.

121 The wild-type ball python colour morph displays a black background with tan-coloured
122 lateral saddles and traces of yellow pigmentation (Figure 1A). Comparing the wild type to the
123 albino colour morph highlights normal xanthophore pigmentation and patterning: in non-
124 axanthic individuals, yellow pigment typically overlaps with the tan-coloured saddles and is
125 absent from the dark melanic regions (Figure 1B). In contrast, axanthic ball pythons lack yellow
126 pigmentation but retain the wild-type melanin pattern (Figure 1C).

127 We extracted and sequenced DNA from the shed skins using a standard three-day
128 phenol-chloroform procedure. DNA quantification and quality checks were performed with an
129 Infinite® 200 Nanoquant (Tecan Group Ltd., Männedorf, Switzerland). After normalizing the
130 DNA from each sample, we combined them into pools in equimolar amounts. These pooled
131 samples (case and controls) were then sent to the McGill Genome Centre for whole-genome
132 sequencing. Library preparation was performed using a PCR-based method, and sequencing
133 was carried out with 150 bp paired-end reads on one lane of the Illumina NovaSeq 6000
134 platform.

135 *Bioinformatics*

136 We used the trim-fastq.pl program from Popoolation (Kofler et al. 2011a) to filter raw reads
137 based on quality (--quality-threshold 20) and length (--min-length 50). This step ensured that
138 each read had a minimum quality score of 20 and a minimum length of 50 bp. We then mapped
139 the filtered reads to a reference genome using the bwa-mem program with default parameters
140 (Li and Durbin, 2009). Since a ball python reference genome is not available, we aligned the
141 reads to both the draft Burmese python reference genome *Pmo2.0* (Castoe et al. 2013) and the

142 more recent chromosome-length Burmese python assembly (*Python molurus bivittatus*-
143 5.0.2_HiC), available at DNAzoo.org. This chromosome-length assembly, based on Hi-C data
144 (Dudchenko et al. 2017; Dudchenko et al. 2018), is aligned to the annotated draft genome
145 (Castoe et al. 2013) and has been used in previous studies to identify colour-related loci
146 (Garcia-Elfring et al. 2023).

147 Next, we converted SAM files to BAM format using SAMtools (Li et al. 2009) and
148 removed reads with a mapping quality below 20 (-q 20). We then generated mpileup and sync
149 formats using SAMtools and Popoolation2 (Kofler et al. 2011b), respectively, before proceeding
150 to variant calling. Variants were called and filtered with bcftools (vcfutils.pl varFilter) using a
151 minimum depth of five (-d 5) and a mapping quality of 20 (-Q 20).

152 We calculated SNP-specific F_{ST} estimates using fst-sliding.pl from Popoolation2 (Kofler et
153 al. 2011b). F_{ST} values were generated for SNP variants in VPI Axanthic (n=5) compared to the
154 control pools. Since the control pools (e.g., Clown, Spider, etc.) lacked axanthic variation, we
155 expected the derived allele to be fixed in the axanthic samples and the reference allele to be
156 fixed in the control pool. A threshold F_{ST} value of 1.0 was used to identify candidate mutations.
157 To confirm the genomic region and candidate mutation of interest, we generated F_{ST} values
158 between the axanthic samples and additional control pools (Spider, n=26; Enchi, n=7; Ivory,
159 n=15; Lavender, n=14).

160 *Variant annotation and identification of polymorphisms and fixed differences*

161

162 We used the software SnpEff (Cingolani et al. 2012) to annotate variants mapped to
163 both the draft and chromosome-length assemblies. SnpEff utilizes a genome assembly and its
164 corresponding General Feature Format (GFF3) file to assess the functional impact of variants on
165 genomic features. For genomic regions showing elevated FST values ("F_{ST} peaks"), we focused
166 on individual variants with an F_{ST} of 1.0, that mapped to protein-coding regions and were
167 predicted to affect gene products. These included nonsense mutations and small indels
168 classified as "high impact," and missense mutations classified as "moderate impact," which
169 were considered candidate mutations.

170 To visualize the position and effect of a candidate mutation on the protein, we used the
171 program Protter (Omasits et al. 2016). We confirmed the candidate variant by PCR amplification
172 and Sanger sequencing of the locus using samples that were not included in the pooled
173 libraries. We validated the candidate loci by Sanger sequencing samples with genotypes
174 inferred from breeder pedigrees. These included inferred heterozygotes (n=10), homozygotes
175 for the derived axanthism-causing allele (i.e., axanthic individuals, n=6), and inferred
176 homozygotes for the wild-type allele (n=10).

177 Primers used to amplify the region surrounding the candidate locus were designed using
178 Primer3 (Kõressaar and Remm, 2007; Kõressaar et al. 2018). The primers used for PCR
179 amplification were as follows:

180 - Forward: 5'- GAAACTTTTGACCAGACTCAGTC

181 - Reverse: 5'- CTTCAATCACCACAGCCACTCC

182 *Synteny and phylogenetic analysis of gch1 and gch2*

183 We conducted a synteny analysis and constructed a phylogenetic tree for the *gch1* and *gch2*
184 genes across multiple species: Burmese python (*Python bivittatus*), brown anole (*Anolis sagrei*),
185 coelacanth (*Latimeria chalumnae*), and the elephant shark (*Callorhinchus milii*). To ensure focus
186 on conserved regions, we trimmed the gene sequences (555 bp) before alignment. Due to the
187 evolutionary divergence of these species, we used MAFFT to build the tree(Katoh et al. 2002).
188 Phylogenetic trees were then built using FastTree (Price et al. 2010), which estimates
189 maximum-likelihood phylogenies, allowing us to infer the evolutionary relationships of these
190 genes across species.

191

192 **RESULTS**

193 Our whole-genome sequencing and variant calling identified 26,449,779 SNPs across all samples
194 received from ball python breeders. Analysis of allele frequency differences between the
195 axanthic pool and the control pool (Clown colour morph) demonstrates overall high levels of
196 background F_{ST}, likely resulting from the low sample size for the axanthic phenotype (n=5). We
197 find two areas of high differentiation or F_{ST} peaks. One region (~24.8 Mb) on chromosome two
198 (Figure 2A) and a second peak on chromosome three, corresponding to the region containing
199 the Clown mutation (Garcia-Elfring et al. *in prep*). Comparing the axanthic data with additional
200 control pools (Spider, n=26; Enchi, n=7; Ivory, n=15; Lavender, n=14) confirms that the region of
201 high differentiation on chromosome two is associated with axanthism (Figure S1). Within the
202 peak on chromosome two, one variant had both high levels of differentiation (F_{ST} = 1) and is

203 predicted to have a high impact on the gene product. This variant is a nonsense mutation, and
204 it maps to exon 5 of LOC103050242 (*GTP cyclohydrolase 1-like*) in the draft assembly. The
205 candidate SNP consists of a C to T nucleotide change (c.520C>T), changing an arginine residue
206 (CGA) to a TGA stop codon (p.Arg174*). This genetic variant is expected to result in a truncated
207 protein (Figure 2B). We validated the axanthic variant found in poolseq data by PCR
208 amplification and Sanger sequencing of the locus of interest in additional individuals (inferred
209 heterozygotes: n=10; homozygotes for the derived axanthism-causing allele: n=6; inferred
210 homozygotes for the wild type allele: n=10). All individuals tested had the genotype that was
211 inferred from pedigrees by breeders.

212 Based on the annotation of *gch1* in the Burmese python reference genome and the
213 absence of an annotated *gch2*, we hypothesized that the gene LOC103050242 (*GTP*
214 *cyclohydrolase 1-like*) corresponds to the paralog *gch2*. A phylogenetic analysis shows that the
215 Burmese python gene LOC103050242 is more closely related to the brown anole
216 LOC132761499 and coelacanth *gch2* than to Burmese python *gch1* (Figure S2). Synteny analysis
217 further supports the identification of LOC103050242 as *gch2*. In humans, coelacanth, and
218 python, *gch1* is flanked by *samd4a*, while in coelacanth and python, *gch2* (LOC103050242 in
219 python) is flanked by *pigf* and *cript* (Figure S3).

220

221 **DISCUSSION**

222 Captive-bred ball pythons have emerged as a valuable model system for studying pigmentation
223 biology, offering unique opportunities to explore the genetics of colouration in reptiles (Brown

224 et al. 2022; Dao et al. 2023; Garcia-Elfring et al. 2023; Lederer et al. 2023). In this study, we
225 focused on an axanthic line of ball pythons to investigate the genetic basis of yellow
226 pigmentation in these snakes. While yellow and red hues in vertebrate integument can arise
227 from dietary carotenoids or endogenous pigments, the carnivorous diet of snakes, combined
228 with the yellow colouration observed in wildtype ball pythons, led us to hypothesize that
229 endogenous pigments are the primary source of yellow colouration in this species. Given the
230 normal melanin pattern seen in axanthic ball pythons, we speculated that any candidate
231 mutation would likely be found in a gene associated with pigment biosynthesis rather than in
232 one related to xanthophore cell-fate specification.

233 Our analysis identified a mutation in *gch2*, a gene known as *ribA* in bacteria, including *E.*
234 *coli*, where it was first isolated and extensively studied (Richter et al. 1993; Averianova et al.
235 2020). *Gch2* plays a critical role in the biosynthesis of riboflavin (vitamin B2) and the production
236 of flavin nucleotide coenzymes, which are vital for numerous enzymatic reactions (Bacher et al.
237 2000; Ren et al. 2005). Unlike animals, bacteria can synthesize riboflavin de novo through an
238 ancestrally conserved pathway, like that found in plants and fungi (Anam et al. 2020;
239 Averianova et al. 2020; Nasuno et al. 2022; Tian et al. 2022). Bacterial studies have shown that
240 *gch2* catalyzes the conversion of GTP into 2,5-diamino-6-ribosyl-amino-4(3H)-pyrimidinedione
241 5′-phosphate (DARPP), releasing formate and pyrophosphate as byproducts (Averianova et al.
242 2020; Klein et al. 2023). In animals, although *gch2* can catalyze the GTP to DARPP reaction, its
243 physiological role is considered non-essential since the riboflavin pathway is not fully
244 functional.

245 The precise function of *gch2* in animals remains less clear compared to that of *gch1*
246 (*GTP cyclohydrolase I*), which is essential for the synthesis of tetrahydrobiopterin (BH4), a
247 cofactor for enzymes involved in neurotransmitter production (e.g., dopamine, serotonin) and
248 nitric oxide synthesis. It also serves as a marker for the xanthophore lineage (Thöny et al. 2000;
249 Ziegler et al. 2000; Pelletier et al. 2001; Nagao et al. 2014; Hamied et al. 2020; Wu et al. 2022).
250 In humans, mutations in *gch1* lead to severe metabolic and neurological disorders (Nagatsu
251 Ichinose, 1996; Longo, 2009; Fanet et al. 2021; Himmelreich et al. 2021), such as
252 phenylketonuria (Trujillano et al. 2017) and DOPA-responsive dystonia (Hirano and Ueno 1999;
253 Yoshino et al. 2018; Kostić et al. 2020; Bradley et al. 2021). *Gch1* and BH4 are also crucial for
254 embryonic development, with homozygous mutations being lethal in mice and zebrafish
255 (Douglas et al. 2015; Larbalestier et al. 2022).

256 Although *gch2* and *gch1* share functional similarities, such as guanine ring opening,
257 formate release, and zinc binding, the reactions they catalyze differ in significant ways
258 (Auerbach et al. 2000; Kaiser et al. 2002; Ren et al. 2005). The role of *gch2* in vertebrate
259 pigmentation is less well understood, but it has been identified as an early marker for
260 xanthophores (Parichy et al. 2000; Miyadai et al. 2023). In zebrafish, *gch2* is essential for larval
261 xanthophore pigmentation but not in adults (Lister, 2019). Conversely, research in flounder
262 suggests that *gch2* is necessary for adult melanophore and xanthophore differentiation
263 (Watanabe et al. 2008).

264 We discovered a nonsense mutation at residue 174 (p.Arg174*), likely resulting in a
265 non-functional protein, occurring 16 residues upstream of the conserved histidine believed to

266 be critical for producing DARPP from GTP (Yadav et al. 2020). Our findings indicate that
267 xanthophore pigmentation in ball pythons arises from the riboflavin biosynthesis pathway,
268 rather than the biopterin pathway. Additionally, since loss-of-function mutations in *gch1* often
269 lead to severe developmental defects, the involvement of *gch2*—rather than *gch1*—is
270 consistent with the absence of pleiotropic effects in axanthic ball pythons.

271 The extensive phenotypic variation in ball python colour morphs and the wide range of
272 colour combinations breeders have produced in captivity provide an opportunity to explore and
273 test hypotheses regarding the mechanisms behind pattern formation. Recent studies suggest
274 that all ball pythons lack iridophores, one of the three chromatophore types (Tzika 2024). This
275 makes ball pythons natural analogs to Shd mutant zebrafish, which also lack iridophores
276 (Frohnhöfer et al., 2013). In addition to axanthism, ball python colour morphs can exhibit
277 xanthism, which is characterized by an increase in yellow brightness (possibly due to melanin
278 changes) or in the distribution of yellow pigment (e.g., the 'Enchi' morph). Many ball python
279 colour morphs that seem to affect melanophore migration (e.g., Tri-Stripe, which shows altered
280 melanin patterns) display xanthophore pigmentation in regions typically covered by dark
281 melanin. This non-overlap of black and yellow pigments suggests that xanthophores and
282 melanophores repel each other, as observed in zebrafish (Frohnhöfer et al., 2013).

283 In zebrafish double mutants (Shd;Pfe), where two of the three chromatophore types
284 (e.g., iridophores and xanthophores) are absent, the remaining chromatophore type (e.g.,
285 melanophores) uniformly covers the body, uninhibited by cell-cell interactions. Similarly, we
286 hypothesize that the genetic basis of all-black melanic ball python morphs, such as ‘Cinnamon’

287 (Figure 1H), is likely due to mutations in genes essential for xanthophore development, allowing
288 melanophores to spread across the body. This contrasts with mutations in melanin production
289 genes, like agouti, which are more common in mammals (e.g., Sasamori et al. 2017; Reissmann
290 et al. 2020). Further support for a repulsive interaction between xanthophores and
291 melanophores comes from the Albino form of the Cinnamon morph (Figure 1I). Instead of
292 revealing an underlying pterin pigment pattern, which might be expected if melanism was
293 driven by excessive melanin production, the 'Cinnamon Albino' phenotype presents as an
294 entirely white ball python with no pterin pigmentation (Figure 1I).

295 Other recessive lines of axanthism exist in captive-bred ball pythons, such as the 'MJ'
296 line. Notably, VPI Axanthic and other axanthism lines are not allelic with one another, meaning
297 crosses between different lines result in double heterozygotes with wildtype coloration,
298 suggesting distinct genetic causes for each axanthism lineage. These various axanthism lines,
299 when combined with other color variants (Figure 1D), provide valuable models to further
300 explore the pterin pigment biosynthesis pathway and identify new axanthism-causing genes in
301 reptiles. Consistent with our findings, we demonstrated in the VPI lineage that pterin pigment
302 metabolism, rather than carotenoid metabolism, is associated with yellow coloration in ball
303 pythons.

304 In summary, our study highlights a significant link between *gch2* and axanthism in ball
305 pythons, suggesting that the initial stages of the ancestral riboflavin pathway are crucial for
306 yellow pigmentation. Further research is necessary to identify the specific xanthophore

307 pigments involved in ball python pigmentation. Nonetheless, our findings enhance the
308 understanding of the genetics of pigmentation in reptiles.

309

310 **CONCLUSION**

311 We used ball python colour morphs to study the genetic basis of xanthophore pigmentation in
312 snakes. We found axanthism is associated with a key gene in the biopterin biosynthesis
313 pathway, providing the first evidence that pterins, not carotenoids, produce the yellow pigment
314 observed in ball pythons. To our knowledge, *gch1* is the first axanthism-associated gene
315 identified in vertebrates. Our results provide new research avenues for the study of axanthism
316 and xanthophore pigmentation in snakes and highlights the utility of using captive-bred ball
317 pythons in pigmentation research.

318 **REFERENCES**

319 Anam, K., Nasuno, R. and Takagi, H., 2020. A novel mechanism for nitrosative stress tolerance
320 dependent on GTP cyclohydrolase II activity involved in riboflavin synthesis of yeast.
321 Scientific Reports, 10(1), p.6015.

322 Andrade, P. and Carneiro, M., 2021. Pterin-based pigmentation in animals. Biology Letters,
323 17(8), p.20210221.

324 Auerbach, G., Herrmann, A., Bracher, A., Bader, G., Gütlich, M., Fischer, M., Neukamm, M.,
325 Garrido-Franco, M., Richardson, J., Nar, H. and Huber, R., 2000. Zinc plays a key role in

326 human and bacterial GTP cyclohydrolase I. Proceedings of the National Academy of
327 Sciences, 97(25), pp.13567-13572.

328 Averianova, L.A., Balabanova, L.A., Son, O.M., Podvolotskaya, A.B. and Tekutyeva, L.A., 2020.
329 Production of vitamin B2 (riboflavin) by microorganisms: an overview. Frontiers in
330 Bioengineering and Biotechnology, 8, p.570828.

331 Bacher, A., Eberhardt, S., Fischer, M., Kis, K. and Richter, G., 2000. Biosynthesis of vitamin b2
332 (riboflavin). Annual review of nutrition, 20(1), pp.153-167.

333 Baltazar-Soares, M., Karell, P., Wright, D., Nilsson, J.Å. and Brommer, J.E., 2024. Genomic basis
334 of melanin-associated phenotypes suggests colour-specific environmental adaptations
335 in tawny owls. *Molecular Ecology*, p.e17247.

336 Barrett, R.D., Laurent, S., Mallarino, R., Pfeifer, S.P., Xu, C.C., Foll, M., Wakamatsu, K., Duke-
337 Cohan, J.S., Jensen, J.D. and Hoekstra, H.E., 2019. Linking a mutation to survival in wild
338 mice. Science, 363(6426), pp.499-504.

339 Bechtel, H.B., 1991. Inherited colour defects: Comparison between humans and snakes.
340 International Journal of Dermatology, 30(4), pp.243-246.

341 Borteiro, C., Diesel Abegg, A., Hirouki Oda, F., Cardozo, D.E., Kolenc, F., Etchandy, I., Bisaiz, I.,
342 Prigioni, C. and Baldo, J.D., 2021. Aberrant colouration in wild snakes: case study in
343 Neotropical taxa and a review of terminology.

Bradley, M., Lyons, S., Coleman, S., Vance, R., Molloy, F. and Widdess-Walsh, P., 2021. A Case of GCH-1 Mutation Dopa-Responsive Dystonia Requiring High Doses of Levodopa for Treatment. Tremor and Other Hyperkinetic Movements, 11.

Brown, A.R., Comai, K., Mannino, D., McCullough, H., Donekal, Y., Meyers, H.C., Graves, C.W., Seidel, H.S. and BIO306W Consortium, 2022. A community-science approach identifies genetic variants associated with three colour morphs in ball pythons (Python regius). Plos one, 17(10), p.e0276376.

Bukowski, L., Erickson, K. and Lyerla, T.A., 1990. Characterization of the yellow pigment in the axanthic mutant of the Mexican axolotl, Ambystoma mexicanum. Pigment Cell Research, 3(3), pp.123-125.

Caro, T., 2017. Wallace on colouration: contemporary perspective and unresolved insights. Trends in ecology & evolution, 32(1), pp.23-30.

Castoe, T.A., De Koning, A.J., Hall, K.T., Card, D.C., Schield, D.R., Fujita, M.K., Ruggiero, R.P., Degner, J.F., Daza, J.M., Gu, W. and Reyes-Velasco, J., 2013. The Burmese python genome reveals the molecular basis for extreme adaptation in snakes. Proceedings of the National Academy of Sciences, 110(51), pp.20645-20650.

Cattaneo, A., 2015. The Zamenis longissimus (Laurenti) axanthic phenotype found on the Castelporziano Presidential Estate: considerations on its morphology, genetic nature and probable extinction (Serpentes: Colubridae). Rendiconti Lincei, 26, pp.385-389.

363 Cavalcante, R. and Bruni, G., 2018. Axanthism in Emys orbicularis hellenica (Valenciennes, 1832)
364 (Testudines: Emydidae) from Piedmont, northern Italy. The Herpetological Bulletin, 146,
365 pp.36-38.

366 Cingolani, P., Platts, A., Wang, L.L., Coon, M., Nguyen, T., Wang, L., Land, S.J., Lu, X. and Ruden,
367 D.M., 2012. A program for annotating and predicting the effects of single nucleotide
368 polymorphisms, SnpEff: SNPs in the genome of Drosophila melanogaster strain w1118;
369 iso-2; iso-3. Fly, 6(2), pp.80-92.

370 Cott, H.B., 1940. Adaptive colouration in animals. Methuen & Co (1940)

371 Courtright, J.B., 1967. Polygenic control of aldehyde oxidase in Drosophila. Genetics, 57(1),
372 p.25.

373 Dao, U.M., Lederer, I., Tabor, R.L., Shahid, B., Graves, C.W. and Seidel, H.S., 2022. Leucism and
374 stripe formation in ball pythons (Python regius) are associated with variants affecting
375 endothelin signaling. bioRxiv.

376 Douglas, G., Hale, A.B., Crabtree, M.J., Ryan, B.J., Hansler, A., Watschinger, K., Gross, S.S.,
377 Lygate, C.A., Alp, N.J. and Channon, K.M., 2015. A requirement for Gch1 and
378 tetrahydrobiopterin in embryonic development. Developmental biology, 399(1), pp.129-
379 138.

380 Dudchenko, O., Batra, S.S., Omer, A.D., Nyquist, S.K., Hoeger, M., Durand, N.C., Shamim, M.S.,
381 Machol, I., Lander, E.S., Aiden, A.P. and Aiden, E.L., 2017. De novo assembly of the

382 Aedes aegypti genome using Hi-C yields chromosome-length scaffolds. Science,
383 356(6333), pp.92-95.

384 Dudchenko, O., Shamim, M.S., Batra, S.S., Durand, N.C., Musial, N.T., Mostofa, R., Pham, M.,
385 Hilaire, B.S., Yao, W., Stamenova, E. and Hoeger, M., 2018. The Juicebox Assembly Tools
386 module facilitates de novo assembly of mammalian genomes with chromosome-length
387 scaffolds for under $1000. BioRxiv, 254797. Preprint.

388 Dunson, M.K., 1974. Ultrastructure of pigment cells in wild type and colour mutants of the
389 Mexican axolotl. Cell and Tissue Research, 151, pp.259-268.

390 Endler, J.A. and Mappes, J., 2017. The current and future state of animal colouration research.
391 Philosophical Transactions of the Royal Society B: Biological Sciences, 372(1724),
392 p.20160352.

393 Evans, B.A. and Howells, A.J., 1978. Control of drosopterin synthesis in Drosophila
394 melanogaster: mutants showing an altered pattern of GTP cyclohydrolase activity during
395 development. Biochemical genetics, 16(1-2), pp.13-26.

396 Fanet, H., Capuron, L., Castanon, N., Calon, F. and Vancassel, S., 2021. Tetrahydrobioterin (BH4)
397 pathway: from metabolism to neuropsychiatry. Current Neuropharmacology, 19(5),
398 pp.591-609.

399 Frohnhöfer, H.G., Krauss, J., Maischein, H.M. and Nüsslein-Volhard, C., 2013. Iridophores and
400 their interactions with other chromatophores are required for stripe formation in
401 zebrafish. Development, 140(14), pp.2997-3007.

402 Frost, S.K., Epp, L.G. and Robinson, S.J., 1986. The pigmentary system of developing axolotls: IV.
403 An analysis of the axanthic phenotype.

404 García-Borrón, J.C., Sánchez-Laorden, B.L. and Jiménez-Cervantes, C., 2005. Melanocortin-1
405 receptor structure and functional regulation. *Pigment cell research*, *18*(6), pp.393-410.

406 Garcia-Elfring, A., Sabin, C.E., Iouchmanov, A.L., Roffey, H.L., Samudra, S.P., Alcala, A.J., Osman,
407 R.S., Lauderdale, J.D., Hendry, A.P., Menke, D.B. and Barrett, R.D., 2023. Piebaldism and
408 chromatophore development in reptiles are linked to the tfec gene. Current Biology,
409 33(4), pp.755-763.

410 Glassman, E. and Mitchell, H.K., 1959. Mutants of Drosophila melanogaster deficient in
411 xanthine dehydrogenase. Genetics, 44(2), p.153.

412 Goto, M. and Sugiura, K., 1971. Biosynthesis of pteridines in Drosophila melanogaster and Rana
413 catesbeiana. In Methods in Enzymology (Vol. 18, pp. 746-761). Academic Press.

414 Hamied, A., Alnedawy, Q., Correia, A., Hacker, C., Ramsdale, M., Hashimoto, H. and Kudoh, T.,
415 2020. Identification and characterization of highly fluorescent pigment cells in embryos
416 of the Arabian killifish (Aphanius Dispar). Iscience, 23(11).

417 Harris, R.B., Irwin, K., Jones, M.R., Laurent, S., Barrett, R.D., Nachman, M.W., Good, J.M.,
418 Linnen, C.R., Jensen, J.D. and Pfeifer, S.P., 2020. The population genetics of crypsis in
419 vertebrates: recent insights from mice, hares, and lizards. Heredity, 124(1), pp.1-14.
420 Soare

421 Himmelreich, N., Blau, N. and Thöny, B., 2021. Molecular and metabolic bases of
422 tetrahydrobiopterin (BH4) deficiencies. Molecular Genetics and Metabolism, 133(2),
423 pp.123-136.

424 Hirano, M. and Ueno, S., 1999. Mutant GTP cyclohydrolase I in autosomal dominant dystonia
425 and recessive hyperphenylalaninemia. Neurology, 52(1), pp.182-182.

426 Hopkins, F.G., 1895. XV. The pigments of the Pieridæ: a contribution to the study of excretory
427 substances which function in ornament. Philosophical Transactions of the Royal Society
428 of London.(B.), (186), pp.661-682.

429 Irion, U., Frohnhöfer, H.G., Krauss, J., Çolak Champollion, T., Maischein, H.M., Geiger-Rudolph,
430 S., Weiler, C. and Nüsslein-Volhard, C., 2014. Gap junctions composed of connexins 41.8
431 and 39.4 are essential for colour pattern formation in zebrafish. Elife, 3, p.e05125.

432 Jablonski, D., Alena, A., Vlček, P. and Jandzik, D., 2014. Axanthism in amphibians: A review and
433 the first record in the widespread toad of the Bufotes viridis complex (Anura:
434 Bufonidae). Belgian Journal of Zoology, 144(2).

435 Kaiser, J., Schramek, N., Eberhardt, S., Püttmer, S., Schuster, M. and Bacher, A., 2002.
436 Biosynthesis of vitamin B2: An essential zinc ion at the catalytic site of GTP
437 cyclohydrolase II. European journal of biochemistry, 269(21), pp.5264-5270.

438 Katoh, K. and Toh, H., 2008. Recent developments in the MAFFT multiple sequence alignment
439 program. *Briefings in bioinformatics*, *9*(4), pp.286-298.

440 Kelsh, R.N., Brand, M., Jiang, Y.J., Heisenberg, C.P., Lin, S., Haffter, P., Odenthal, J., Mullins,
441 M.C., Van Eeden, F.J., Furutani-Seiki, M. and Granato, M., 1996. Zebrafish pigmentation
442 mutations and the processes of neural crest development. Development, 123(1),
443 pp.369-389.

444 Kikuchi, D.W. and Pfennig, D.W., 2012. A Batesian mimic and its model share colour production
445 mechanisms. Current Zoology, 58(4), pp.658-667.

446 Kikuchi, D.W., Seymoure, B.M. and Pfennig, D.W., 2014. Mimicry's palette: widespread use of
447 conserved pigments in the aposematic signals of snakes. Evolution & Development,
448 16(2), pp.61-67.

449 Kim, H., Kim, K. and Yim, J., 2013. Biosynthesis of drosopterins, the red eye pigments of
450 Drosophila melanogaster. IUBMB life, 65(4), pp.334-340.

451 Klein, V.J., Brito, L.F., Perez-Garcia, F., Brautaset, T. and Irla, M., 2023. Metabolic engineering of
452 thermophilic Bacillus methanolicus for riboflavin overproduction from methanol.
453 Microbial Biotechnology, 16(5), pp.1011-1026.

454 Kofler, R., Orozco-terWengel, P., De Maio, N., Pandey, R.V., Nolte, V., Futschik, A., Kosiol, C. and
455 Schlötterer, C., 2011a. PoPoolation: a toolbox for population genetic analysis of next
456 generation sequencing data from pooled individuals. PloS one, 6(1), p.e15925.

457 Kofler, R., Pandey, R.V. and Schlötterer, C., 2011b. PoPoolation2: identifying differentiation
458 between populations using sequencing of pooled DNA samples (Pool-Seq).
459 Bioinformatics, 27(24), pp.3435-3436.

460 Kolenda, K., Najbar, B., Najbar, A., Kaczmarek, P., Kaczmarski, M. and Skawiński, T., 2017. Rare
461 colour aberrations and anomalies of amphibians and reptiles recorded in Poland.
462 Herpetology Notes, 10, pp.103-109.

463 Kõressaar, T. and Remm, M., 2007. Enhancements and modifications of primer design program
464 Primer3. Bioinformatics, 23(10), pp.1289-1291.

465 Kõressaar, T., Lepamets, M., Kaplinski, L., Raime, K., Andreson, R. and Remm, M., 2018.
466 Primer3_masker: integrating masking of template sequence with primer design
467 software. Bioinformatics, 34(11), pp.1937-1938.

468 Kostić, V.S., Agosta, F., Tomic, A., Sarasso, E., Kresojevic, N., Basaia, S., Svetel, M., Copetti, M.
469 and Filippi, M., 2020. Brain structural alterations in patients with GCH1 mutations
470 associated DOPA-responsive dystonia. Journal of Neurology, Neurosurgery & Psychiatry.

471 Kronforst, M.R., Barsh, G.S., Kopp, A., Mallet, J., Monteiro, A., Mullen, S.P., Protas, M.,
472 Rosenblum, E.B., Schneider, C.J. and Hoekstra, H.E., 2012. Unraveling the thread of
473 nature's tapestry: the genetics of diversity and convergence in animal pigmentation.
474 Pigment cell & melanoma research, 25(4), pp.411-433.

475 Larbalestier, H., Keatinge, M., Watson, L., White, E., Gowda, S., Wei, W., Koler, K., Semenova,
476 S.A., Elkin, A.M., Rimmer, N. and Sweeney, S.T., 2022. GCH1 deficiency activates brain
477 innate immune response and impairs tyrosine hydroxylase homeostasis. Journal of
478 Neuroscience, 42(4), pp.702-716.

479 Lederer, I., Shahid, B., Dao, U., Brogdon, A., Byrtus, H., Delva, M., Deva, O., Hatfield, P., Hertz,
480 M., Justice, J. and Mavor, S., 2023. A frameshift variant in the melanophilin gene is
481 associated with loss of pigment from shed skin in ball pythons (Python regius).
482 Micropublication Biology, 2023.

483 Li, H. and Durbin, R., 2009. Fast and accurate short read alignment with Burrows–Wheeler
484 transform. bioinformatics, 25(14), pp.1754-1760.

485 Li, H., Handsaker, B., Wysoker, A., Fennell, T., Ruan, J., Homer, N., Marth, G., Abecasis, G. and
486 Durbin, R., 2009. The sequence alignment/map format and SAMtools. Bioinformatics,
487 25(16), pp.2078-2079.

488 Lister, J.A., 2019. Larval but not adult xanthophore pigmentation in zebrafish requires GTP
489 cyclohydrolase 2 (gch2) function. Pigment Cell & Melanoma Research, 32(5), pp.724-
490 727.

491 Longo, N., 2009. Disorders of biopterin metabolism. Journal of inherited metabolic disease, 32,
492 pp.333-342.

493 Lyerla, T.A. and Dalton, H.C., 1971. Genetic and developmental characteristics of a new colour
494 variant, axanthic, in the Mexican axolotl, Ambystoma mexicanum Shaw. Developmental
495 Biology, 24(1), pp.1-18.

496 Maoka, T., 2020. Carotenoids as natural functional pigments. Journal of natural medicines,
497 74(1), pp.1-16.

498 Masselink, W. and Tanaka, E.M., 2021. Toward whole tissue imaging of axolotl regeneration.
499 Developmental Dynamics, 250(6), pp.800-806.

500 McNamara, M.E., Rossi, V., Slater, T.S., Rogers, C.S., Ducrest, A.L., Dubey, S. and Roulin, A.,
501 2021. Decoding the evolution of melanin in vertebrates. Trends in Ecology & Evolution.

502 Miyadai, M., Takada, H., Shiraishi, A., Kimura, T., Watakabe, I., Kobayashi, H., Nagao, Y., Naruse,
503 K., Higashijima, S.I., Shimizu, T. and Kelsh, R.N., 2023. A gene regulatory network
504 combining Pax3/7, Sox10 and Mitf generates diverse pigment cell types in medaka and
505 zebrafish. Development, 150(19).

506 Minchin, J.E. and Hughes, S.M., 2008. Sequential actions of Pax3 and Pax7 drive xanthophore
507 development in zebrafish neural crest. Developmental biology, 317(2), pp.508-522.

508 Morgan, T.H., 1910. Sex limited inheritance in Drosophila. Science, 32(812), pp.120-122.

509 Nagao, Y., Suzuki, T., Shimizu, A., Kimura, T., Seki, R., Adachi, T., Inoue, C., Omae, Y., Kamei, Y.,
510 Hara, I. and Taniguchi, Y., 2014. Sox5 functions as a fate switch in medaka pigment cell
511 development. PLoS genetics, 10(4), p.e1004246.

512 Nagatsu, T. and Ichinose, H., 1996. GTP cyclohydrolase I gene, tetrahydrobiopterin, and tysorine
513 hydroxylase gene: Their relations to dystonia and parkinsonism. Neurochemical
514 research, 21, pp.245-250.

515 Nasuno, R., Suzuki, S., Oiki, S., Hagiwara, D. and Takagi, H., 2022. Identification and Functional
516 Analysis of GTP Cyclohydrolase II in Candida glabrata in Response to Nitrosative Stress.
517 Frontiers in Microbiology, 13, p.825121.

518 Odenthal, J., Rossnagel, K., Haffter, P., Kelsh, R.N., Vogelsang, E., Brand, M., van Eeden, F.J.,
519 Furutani-Seiki, M., Granato, M., Hammerschmidt, M. and Heisenberg, C.P., 1996.
520 Mutations affecting xanthophore pigmentation in the zebrafish, Danio rerio.
521 Development, 123(1), pp.391-398.

522 Omasits, U., Ahrens, C.H., Müller, S. and Wollscheid, B., 2014. Protter: interactive protein
523 feature visualization and integration with experimental proteomic data. Bioinformatics,
524 30(6), pp.884-886.

525 Owen, J.P., Kelsh, R.N. and Yates, C.A., 2020. A quantitative modelling approach to zebrafish
526 pigment pattern formation. *Elife*, *9*, p.e52998.

527 Parichy, D.M., Ransom, D.G., Paw, B., Zon, L.I. and Johnson, S.L., 2000. An orthologue of the kit-
528 related gene fms is required for development of neural crest-derived xanthophores and
529 a subpopulation of adult melanocytes in the zebrafish, Danio rerio. Development,
530 127(14), pp.3031-3044.

531 Pelletier, I., Bally-Cuif, L. and Ziegler, I., 2001. Cloning and developmental expression of
532 zebrafish GTP cyclohydrolase I. Mechanisms of development, 109(1), pp.99-103.

533 Price, M.N., Dehal, P.S. and Arkin, A.P., 2010. FastTree 2–approximately maximum-likelihood
534 trees for large alignments. *PloS one*, *5*(3), p.e9490.

535 Reaume, A.G., Knecht, D.A. and Chovnick, A., 1991. The rosy locus in Drosophila melanogaster:
536 xanthine dehydrogenase and eye pigments. Genetics, 129(4), pp.1099-1109.

537 Reissmann, M., Ullrich, E., Bergfeld, U. and Ludwig, A., 2024. Agouti-Signaling Protein and
538 Melanocortin-1-Receptor Mutations Associated with Coat Color Phenotypes in Fallow
539 Deer (Dama dama). Genes, 15(8), p.1055.

540 Ren, J., Kotaka, M., Lockyer, M., Lamb, H.K., Hawkins, A.R. and Stammers, D.K., 2005. GTP
541 cyclohydrolase II structure and mechanism. Journal of Biological Chemistry, 280(44),
542 pp.36912-36919.

543 Richter, G., Ritz, H., Katzenmeier, G., Volk, R., Kohnle, A., Lottspeich, F., Allendorf, D. and
544 Bacher, A., 1993. Biosynthesis of riboflavin: cloning, sequencing, mapping, and
545 expression of the gene coding for GTP cyclohydrolase II in Escherichia coli. Journal of
546 bacteriology, 175(13), pp.4045-4051.

547 San-Jose, L.M. and Roulin, A., 2017. Genomics of colouration in natural animal populations.
548 Philosophical Transactions of the Royal Society B: Biological Sciences, 372(1724),
549 p.20160337.

550 Sasamori, S., Wiewel, A.S., Thomson, V.A., Kobayashi, M., Nakata, K. and Suzuki, H., 2017.
551 Potential causative mutation for melanism in rats identified in the agouti signaling
552 protein gene (Asip) of the Rattus rattus species complex on Okinawa Island,
553 Japan. *Zoological science*, *34*(6), pp.513-522.

554 Schluckebier, R., Sachs, M. and Vences, M., 2022. Axanthic green toads, Bufotes viridis (Anura:
555 Bufonidae), from Cologne, Germany. Herpetology Notes, 15, pp.345-348.

556 Singh, A.P. and Nüsslein-Volhard, C., 2015. Zebrafish stripes as a model for vertebrate colour
557 pattern formation. *Current Biology*, *25*(2), pp.R81-R92.

558 Spradling, A.C. and Rubin, G.M., 1983. The effect of chromosomal position on the expression of
559 the Drosophila xanthine dehydrogenase gene. Cell, 34(1), pp.47-57.

560 Steingrímsson, E., Copeland, N.G. and Jenkins, N.A., 2006. Mouse coat colour mutations: from
561 fancy mice to functional genomics. *Developmental Dynamics: An Official Publication of*
562 *the American Association of Anatomists*, *235*(9), pp.2401-2411.

563 Thöny, B., Auerbach, G. and Blau, N., 2000. Tetrahydrobiopterin biosynthesis, regeneration and
564 functions. Biochemical Journal, 347(1), pp.1-16.

565 Tian, Q., Wang, G., Ma, X., Shen, Q., Ding, M., Yang, X., Luo, X., Li, R., Wang, Z., Wang, X. and Fu,
566 Z., 2022. Riboflavin integrates cellular energetics and cell cycle to regulate maize seed
567 development. Plant Biotechnology Journal, 20(8), pp.1487-1501.

568 Trujillano, D., Perez, B., González, J., Tornador, C., Navarrete, R., Escaramis, G., Ossowski, S.,
569 Armengol, L., Cornejo, V., Desviat, L.R. and Ugarte, M., 2014. Accurate molecular
570 diagnosis of phenylketonuria and tetrahydrobiopterin-deficient hyperphenylalaninemias
571 using high-throughput targeted sequencing. European Journal of Human Genetics,
572 22(4), pp.528-534.*f*

573 Tzika, A.C., 2024. On the role of TFEC in reptilian colouration. Frontiers in Cell and
574 Developmental Biology, 12, p.1358828.

575 Wakamatsu, K. and Ito, S., 2021. Melanins in vertebrates. Pigments, pigment cells and pigment
576 patterns, pp.45-89.

577 Watanabe, K., Washio, Y., Fujinami, Y., Aritaki, M., Uji, S. and Suzuki, T., 2008. Adult-type
578 pigment cells, which colour the ocular sides of flounders at metamorphosis, localize as
579 precursor cells at the proximal parts of the dorsal and anal fins in early larvae.
580 Development, growth & differentiation, 50(9), pp.731-741.

581 Wu, S., Huang, J., Li, Y., Zhao, L. and Liu, Z., 2022. Analysis of yellow mutant rainbow trout
582 transcriptomes at different developmental stages reveals dynamic regulation of skin
583 pigmentation genes. Scientific Reports, 12(1), p.256.

584 Yadav, S., Shinde, R.N., Singh, S., Karthikeyan, S. and Singh, B., 2022. Structurally disordered C-
585 terminal residues of GTP cyclohydrolase II are essential for its enzymatic activity. Journal
586 of Biomolecular Structure and Dynamics, 40(19), pp.9318-9331.

587 Yoshino, H., Nishioka, K., Li, Y., Oji, Y., Oyama, G., Hatano, T., Machida, Y., Shimo, Y., Hayashida,
588 A., Ikeda, A. and Mogushi, K., 2018. GCH1 mutations in dopa-responsive dystonia and
589 Parkinson's disease. Journal of neurology, 265, pp.1860-1870.

590 Ziegler, I. and Harmsen, R., 1970. The biology of pteridines in insects. In Advances in insect
591 physiology (Vol. 6, pp. 139-203). Academic Press.

592 Ziegler, I., 2003. The pteridine pathway in zebrafish: regulation and specification during the
593 determination of neural crest cell-fate. Pigment cell research, 16(3), pp.172-182.

Ziegler, I., McDonaldo, T., Hesslinger, C., Pelletier, I. and Boyle, P., 2000. Development of the pteridine pathway in the zebrafish, Danio rerio. Journal of Biological Chemistry, 275(25), pp.18926-18932.

Acknowledgments

We thank Douglas Menke and Benjamin Wortman for discussions on gene phylogeny and synteny. This work was supported by an NSERC Discovery Grant and Canada Research Chair to RDHB and APH. We thank Mutation Creation, T Dot Exotics, The Ball Room Canada, Ball Python Genetics Canada, and Designing Morphs for supplying samples.

Data accessibility

The data that support the findings of this manuscript have been uploaded to the NCBI Sequence Read Archive (SRA) with the accession PRJNA1122856.

Contributions

AGE, APH, and RDHB conceived and designed the study. HR collected samples. AGE and JMA performed the molecular work and AGE the bioinformatics and data analyses. HR performed PCR and Sanger sequencing analysis. AGE wrote the manuscript with input from APH, HR, JMA, and RDHB.

613

A

B

C

D

E

F

G

H

I

Figure 1. Mendelian phenotypes (colour morphs) in ball pythons. Compared to the (A) wild type, (B) the albino colour morph lacks melanin pigment which allows the display of xanthophore (pterin) pigmentation and patterning, occupying the tan-coloured parts of the wild type. (C) The VPI Axanthic is characterized by a lack of yellow pigmentation on a wildtype pattern. (D) Combining colour morphs with axanthism (VPI Axanthic + Pastel + Fire is shown) can create different forms of the colour anomaly. (E) Some colour morphs like Enchi (Albino + Enchi is shown) are associated with changes in xanthophore migration (e.g., xanthism). (F) Tri-Stripe colour morph exhibits altered melanin patterning. (G) The Albino form of Tri-Stripe shows the effects of this colour morph on xanthophore pigmentation. (H) Melanic colour morphs like Cinnamon do not have xanthophore pigmentation, as shown by an (I) all-white snake in the Albino form. Photo credit: worldofballpythons.com

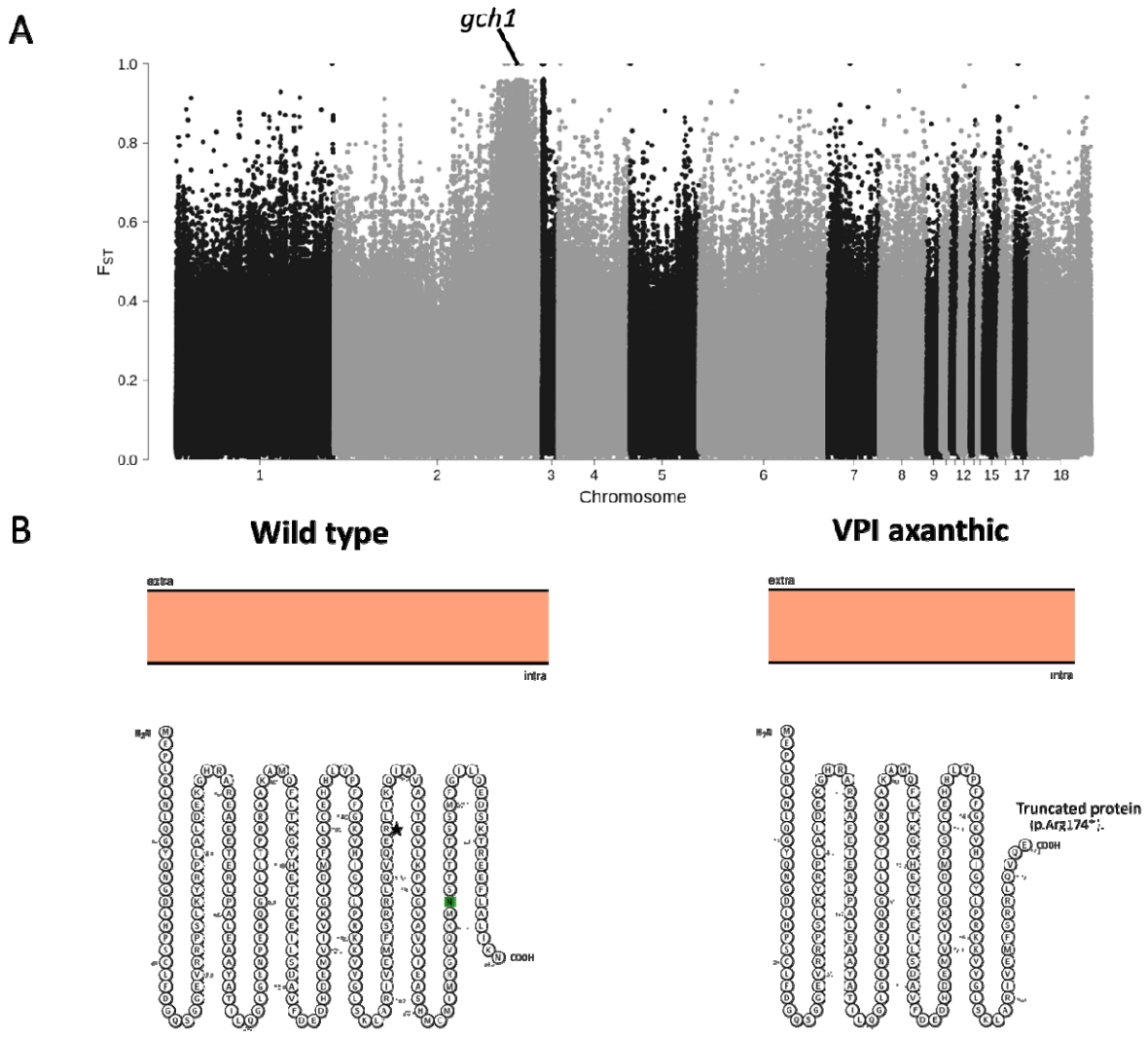

Figure 2. (A) Manhattan plot of F_{ST} values for SNPs mapped to the chromosome-length assembly. Genomic differentiation between VPI axanthic and a reference pool (Clown colour morph) shows a peak on chromosome two housing the axanthism candidate variant on LOC103050242 (*gch2*). (B) Burmese python amino acid sequence of LOC103050242, with the VPI Axanthic locus indicated by an asterisk (left panel). A nonsense mutation the on the 174th residue (p.Arg174*) likely leads to a defective truncated protein (right panel) and axanthism.